Available online at www.sciencedirect.com

SciVerse ScienceDirect

Ceramics International 39 (2013) 2083–2091

CERAMICS INTERNATIONAL

www.elsevier.com/locate/ceramint

Effect of alkaline earth additives on the flexural strength of silicon oxycarbide-bonded silicon carbide ceramics

Jung-Hye Eom[a], Young-Wook Kim[a,*], Byung Jun Jung[b]

[a]*Functional Ceramics Laboratory, Department of Materials Science and Engineering, The University of Seoul, Seoul 130-743, Republic of Korea*
[b]*Organic Electronics Materials Laboratory, Department of Materials Science and Engineering, The University of Seoul, Seoul 130-743, Republic of Korea*

Received 17 July 2012; accepted 23 August 2012
Available online 30 August 2012

Abstract

A series of silicon oxycarbide (SiOC)-bonded SiC ceramics were fabricated from SiC–polysiloxane–alkaline earth (AE) alkoxide mixtures at a temperature as low as 800 °C to investigate the compositional effect on the flexural strength of SiOC-bonded SiC ceramics. The addition of AE elements increased the flexural strength of SiOC-bonded SiC ceramics by 14–65% depending on the composition. The flexural strength versus the Ba/(Ba+Si) mole ratio curve had a maximum in that there was a small composition range for which an optimum flexural strength occurred. The best result, a flexural strength of >150 MPa, was obtained when the ratio was ~0.01.

Keywords: A. Precursors: organic; B. Porosity; D. SiC; Silicon oxycarbide

1. Introduction

Polymer derived ceramics (PDCs) based on Si–O–C (silicon oxycarbide, SiOC) have attracted attention because of their inherent chemical durability [1,2], low processing temperature (1000–1200 °C) [3–10], excellent mechanical strength despite the amorphous phase [11–14], excellent thermal shock resistance [15], creep resistance better than vitreous silica [16,17], and the highest ceramic yield among PDCs [18]. SiOC ceramics have been used as a bonding phase for SiC, but studies using SiOC as a bonding phase for SiC are quite limited. Zhu et al. [19] fabricated polycarbosilane-derived SiC-bonded SiC ceramics with porosities ranging from 44% to 53%. Ma et al. [20] fabricated silicone resin-derived SiOC-bonded SiC ceramics with porosities ranging from 41% to 50%. Thunemann et al. [6] fabricated porous SiC preforms for metal infiltration by intergranular binding with preceramic polymers. However, the heat-treatment temperatures used in these studies were ≥1000 °C, and the resulting ceramics had poor mechanical properties (flexural strengths of 3–22 MPa) [19,20]. Eom and Kim [21] recently demonstrated significant interfacial adhesion between SiC and SiOC phases and reported a flexural strength of 82 MPa when SiOC-bonded SiC ceramics were heat-treated for 1 h at a temperature as low as 800 °C in nitrogen.

Modification of SiOC chemistry by incorporating elements or fillers into the SiOC structure is a method to improve the mechanical properties of the SiOC-bonded SiC ceramics [22,23]. Klonczynski et al. [5] prepared Si(B)CO ceramics by incorporating SiO_2/B_2O_3 fillers into polysiloxane. The addition of boron led to the enhanced crystallization of β-SiC in the oxycarbide matrix and finely dispersed β-SiC nanoparticles embedded in a high temperature-stable, amorphous borosilicate glass structure. Harshe et al. [24] modified polysiloxane by incorporating an Al-containing alkoxide compound to prepare Si(Al)OC ceramics. The Si(Al)OC ceramics showed improved high temperature stability compared to Al-free SiOC compositions. Toma et al. [25] modified polysiloxane by incorporating nano-Al filler and fabricated SiC–mullite–Al_2O_3-based nanocomposites. Fukushima et al. [26] prepared Si–Nb–C–O ceramics through the pyrolysis of an organic–inorganic hybrid gel prepared using methyltriethoxysilane and niobium pentaethoxide. The Si–Nb–C–O ceramics pyrolyzed at 1000 °C showed better oxidation resistance than that heated

*Corresponding author. Tel.: +82 2 2210 2760; fax: +82 2 2215 5863.
E-mail address: ywkim@uos.ac.kr (Y.-W. Kim).

0272-8842/$ - see front matter © 2012 Elsevier Ltd and Techna Group S.r.l. All rights reserved.
http://dx.doi.org/10.1016/j.ceramint.2012.08.064

at lower temperature because of the formation of SiO_2 and an oxycarbide layer at the surface after oxidation. Ionescu et al. [27,28] prepared SiOC–HfO_2 nanocomposites via chemical modification of a polysilsesquioxane by hafnium tetra(*n*-butoxide). The nanocomposites showed a significant improvement in thermal stability with respect to carbothermal decomposition, which is a consequence of the solid-state reaction of hafnia with amorphous silica to generate hafnon ($HfSiO_4$). Bergero et al. [29] added $MoSi_2$ into methyltriethoxysilane and fabricated $MoSi_2$–SiOC composites. The composites displayed good thermal shock resistance, $\Delta T_c > 400$ °C, which was caused by the combination of low Young's modulus and reasonably high flexural strength of the $MoSi_2$–SiOC composites.

A new approach that has received less attention is the incorporation of alkaline-earth (AE) elements in SiOC. Liu et al. [30] added barium–strontium aluminosilicate (BSAS) powder into polysiloxane as filler. After a heat-treatment of C/SiC composites coated with BSAS–polysiloxane at 1350 °C for 2 h in argon, the coating material was oxidation-resistant at 1250 °C in dry air and corrosion-resistant at the same temperature in water vapor.

The aim of the present work is to investigate the effect of AE elements addition on the flexural strength of SiOC-bonded SiC ceramics. The incorporation of AE elements in SiOC glass may provide a new opportunity for improving mechanical properties of SiOC-bonded SiC ceramics.

2. Experimental

Commercially available α-SiC powders (~0.45 μm, A-1, Showa Denko, Tokyo, Japan), polysiloxane (YR3370, GE Toshiba Silicones Co. Ltd., Japan), magnesium tert-butoxide ($Mg(OC(CH_3)_3)_2$, Alfa Aesar, Johnson Matthey Co., Ltd., Ward Hill, MA, USA), calcium methoxide ($Ca(OCH_3)_2$, Sigma-Aldrich Inc., St. Louis, MO, USA), strontium isopropoxide ($Sr(OCH(CH_3)_2)_2$, Alfa Aesar, Johnson Matthey Co., Ltd., Ward Hill, MA, USA), and barium isopropoxide ($Ba(OCH(CH_3)_2)_2$, Alfa Aesar, Johnson Matthey Co., Ltd., Ward Hill, MA, USA) were used as starting materials. The effect of the AE composition was examined by preparing four batches containing 1% AE elements, i.e., AE/(AE+Si) mole ratio = 0.01 in the bonding phase. A base-line material without AE elements was also prepared for comparison.

To investigate the effect of the Ba content, five batches were mixed containing 80 wt% SiC and 20 wt% polysiloxane–Ba isopropoxide with variations in the Ba/(Ba+Si) mole ratio ranging from 0.005 to 0.20 (Table 1). All the batches were separately mixed in polypropylene jars for 16 h using ethanol and SiC balls. The milled slurry was dried, sieved, uniaxially pressed under 50 MPa, and cold pressed isostatically under 345 MPa. Before the pyrolysis process, the polysiloxane in the compacts were cross-linked by heating the specimens to 200 °C in air. The resulting specimens were then heat-treated at 800 °C for 2 h in nitrogen at a heating rate of 1 °C/min. The heat treatment allowed for polysiloxane-to-SiOC conversion, resulting in SiOC-bonded SiC ceramics.

The bulk density of the resulting ceramics was calculated from the weight-to-volume ratio of the samples. The true density of the SiOC material after heat-treatment was measured using a pycnometer for the powdered samples. Crystalline phases in the heat-treated samples were determined via X-ray diffractometry (XRD). The fracture surfaces were observed by scanning electron microscopy. For the flexural strength measurements, bar-shaped samples were cut to a size of 4 mm × 5 mm × 35 mm. Bend tests were performed at room temperature on 4–8 samples under each condition using a three-point method with a span of 30 mm and a crosshead speed of 0.5 mm/min.

To investigate the effect of Ba on the bonding characteristics in the bonding phase, five batches were mixed, each containing polysiloxane and Ba isopropoxide with variations in the Ba/(Ba+Si) mole ratio (Table 2). All the batches were separately mixed in polypropylene jars for 16 h using ethanol and SiC balls. The milled slurry was dried, sieved, thermally cross-linked by heating the specimens to 200 °C in air, and pyrolyzed at 700–900 °C for 2 h in nitrogen with a heating rate of 1 °C/min. Fourier transform infrared (FT-IR) spectra of selected SiOC-bonded SiC ceramics and Ba-modified

Table 1
Batch composition and sample designation of AE-modified SiOC-bonded SiC ceramics.

Sample designation	Composition (wt%)	AE/(AE+Si) mole ratio
SC	α-SiC[a] + 20% polysiloxane[b]	0
SC–1Mg	α-SiC[a] + 19.58% polysiloxane + 0.42% magnesium tert-butoxide ($Mg(OC(CH_3)_3)_2$)[c]	0.01 (AE = Mg)
SC–1Ca	α-SiC + 19.74% polysiloxane + 0.26% calcium methoxide ($Ca(OCH_3)_2$)[d]	0.01 (AE = Ca)
SC–1Sr	α-SiC + 19.49% polysiloxane + 0.51% strontium isopropoxide ($Sr(OCH(CH_3)_2)_2$)[c]	0.01 (AE = Sr)
SC–0.5Ba	α-SiC + 19.68% polysiloxane + 0.32% barium isopropoxide ($Ba(OCH(CH_3)_2)_2$)[c]	0.005 (AE = Ba)
SC–1Ba	α-SiC + 19.37% polysiloxane + 0.63% barium isopropoxide ($Ba(OCH(CH_3)_2)_2$)[c]	0.01 (AE = Ba)
SC–2Ba	α-SiC + 18.77% polysiloxane + 1.23% barium isopropoxide ($Ba(OCH(CH_3)_2)_2$)[c]	0.02 (AE = Ba)
SC–5Ba	α-SiC + 17.11% polysiloxane + 2.89% barium isopropoxide ($Ba(OCH(CH_3)_2)_2$)[c]	0.05 (AE = Ba)
SC–20Ba	α-SiC + 11.09% polysiloxane + 8.91% barium isopropoxide ($Ba(OCH(CH_3)_2)_2$)[c]	0.20 (AE = Ba)

[a] ~0.45 μm, A-1, Showa Denko, Tokyo, Japan.
[b] YR3370, GE Toshiba Silicones Co. Ltd., Tokyo, Japan.
[c] Alfa Aesar, Johnson Matthey Co., Ltd., Ward Hill, MA, USA.
[d] Sigma-Aldrich Inc., St. Louis, MO, USA.

Table 2
Batch composition and sample designation of SiOC and SiOC modified with barium.

Sample designation	Composition (wt%)	Ba/(Ba+Si) mole ratio
SiOC	100% polysiloxane[a]	0
SiOC–1Ba	96.85% polysiloxane+3.15% barium isopropoxide ($Ba(OCH(CH_3)_2)_2$)[b]	0.01
SiOC–5Ba	85.55% polysiloxane+14.45% barium isopropoxide ($Ba(OCH(CH_3)_2)_2$)[b]	0.05
SiOC–20Ba	55.45% polysiloxane+44.55% barium isopropoxide ($Ba(OCH(CH_3)_2)_2$)[b]	0.20
SiOC–80Ba	9.15% polysiloxane+90.85% barium isopropoxide ($Ba(OCH(CH_3)_2)_2$)[b]	0.80

[a]YR3370, GE Toshiba Silicones Co. Ltd., Tokyo, Japan.
[b]Alfa Aesar, Johnson Matthey Co., Ltd., Ward Hill, MA, USA.

SiOC ceramics were measured with a FT-IR spectrometer (ABB FTLA2000, Wickliffe, OH, USA) using KBr pellets.

3. Results and discussion

3.1. Compositional effect

Pyrolysis of the polysiloxane at 800 °C in an inert atmosphere yielded amorphous SiOC with a weight loss of 13% [31,32]. Details of the pyrolysis behavior of the polysiloxane are reported by Narisawa et al. [32]. The effect of AE elements on the pyrolyzed density of samples heat-treated at 800 °C for 2 h is shown in Fig. 1. The density after heat-treatment varied from 2.35 to 2.41 g/cm^3 with a variation in the AE composition. The SC–1Mg sample showed a maximum density of 2.41 g/cm^3, whereas the SC sample containing no AE elements showed the lowest density of 2.35 g/cm^3 after pyrolysis at 800 °C for 2 h in nitrogen. The addition of the AE element slightly increased the density of SiOC-bonded SiC ceramics. The true density of polysiloxane-derived SiOC after the 800 °C heat-treatment was 1.76 ± 0.01 g/cm^3 [21]. The porosity also decreased with the addition of AE elements from 16.6% to 14.7–16.2%, depending on the AE composition (Fig. 1). The densification due to polysiloxane addition was caused by the elimination of residual pores by viscous flow of polysiloxane-derived SiOC modified with AE elements after heat-treatment [21,24]. The incorporation of carbon into the silica network decreased the mobility of the residual vitreous silica network at the molecular level, resulting in a more rigid structure than silica glass [33]. Our results suggest that the incorporation of AE elements into the SiOC network increases the mobility of the residual vitreous SiOC network at the molecular level, resulting in enhanced densification, i.e., decreased porosity.

Fig. 2 shows the typical microstructures of SiOC-bonded SiC ceramics containing 20 wt% polysiloxane with or without AE-alkoxides. As shown in Fig. 2, submicron SiC particles were well bonded to each other by polysiloxane-derived SiOC or polysiloxane-derived SiOC modified with AE. A significant difference in the fracture surface was not observed. Previous work on SiOC-bonded SiC ceramics produced severe cracking in the SiOC bonding phase when large SiC particles (10 or 15 μm) were used [21]. The greater volume reduction of the SiOC phase and constrained coarse

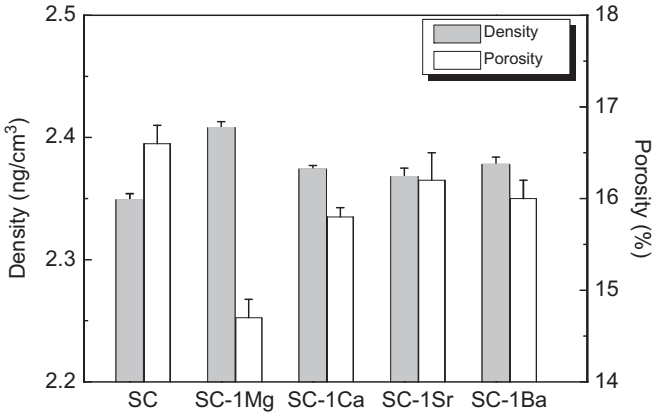

Fig. 1. Density and porosity of polysiloxane-derived SiOC-bonded SiC ceramics (refer to Table 1).

SiC network caused tension within the structure, which resulted in cracking in the specimens [6]. Since finer α-SiC powders (~0.45 μm) were used in the present study, no such micro- or macro-cracks were observed in the fracture surfaces of the samples.

The flexural strength of samples with or without 1% AE elements is shown in Fig. 3. All samples with 1% AE elements showed greater strength than the SC sample without AE. The SC–1Ba sample showed the greatest flexural strength of 153 MPa among the samples investigated. The SC–1Mg sample showed the second greatest strength of 140 MPa. The flexural strengths of SC–1Ba and SC–1Mg samples were 65% and 52% greater than the SC sample without AE elements (93 MPa). Direct bonding between the SiC and SiOC phases was responsible for the strength obtained in the SC sample [21,34], even though the heat-treatment temperature was as low as 800 °C. Possible causes of the improved flexural strength achieved by adding AE-alkoxide are (1) the enhanced densification in AE-modified SiOC-bonded SiC ceramics and (2) stronger bonding between the SiC and AE-modified SiOC than that between SiC and SiOC. The AE element incorporation in SiOC resulted in improved densification (1–2% decrease in porosity), as shown in Fig. 1. The improved densification is caused by the decrease in viscosity of the SiOC glass. If the enhanced densification is the primary factor affecting the flexural strength, a large increase in the flexural strength is not expected considering the general

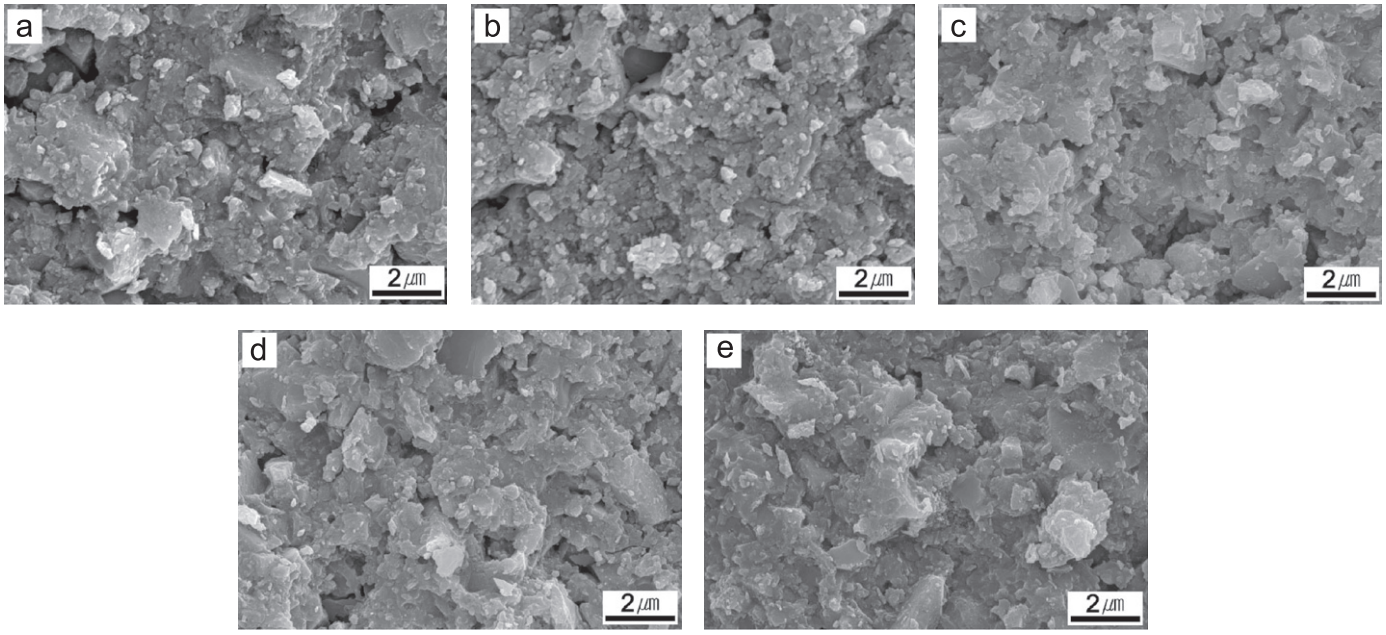

Fig. 2. Typical fracture surfaces of the polysiloxane-derived SiOC-bonded SiC ceramics: (a) SC, (b) SC–1Mg, (c) SC–1Ca, (d) SC–1Sr, and (e) SC–1Ba (refer to Table 1).

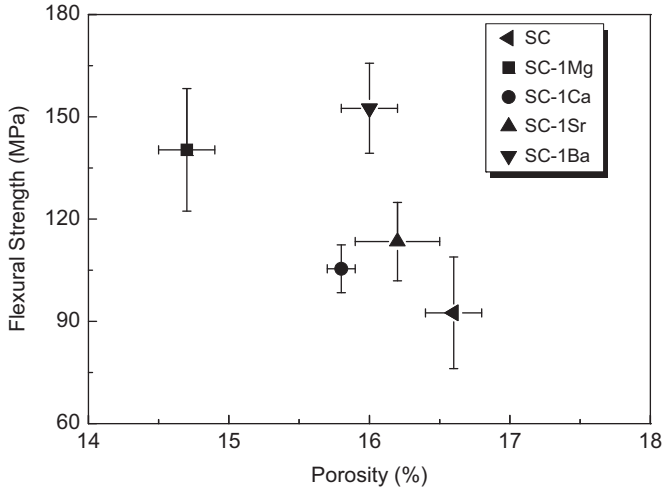

Fig. 3. Flexural strength as a function of the porosity of the polysiloxane-derived SiOC-bonded SiC ceramics.

trend in the porosity-dependency of strength for porous ceramics [10,35–37]. However, Fig. 3 shows that the flexural strength increased from 93 MPa for the SC sample to 105–153 MPa for the AE-modified SiOC-bonded SiC ceramics, depending on the AE composition. Thus, the large increase (13–65%) in the flexural strength was caused by stronger bonding between the SiC and AE-modified SiOC. The difference in flexural strength among AE-modified SiC ceramics was attributed to the difference in chemistry. It is well documented that the interface strength of SiC ceramics is affected by the chemistry of the intergranular phase, i.e., a bonding phase [38].

The flexural strength of the SC sample without AE elements was 93 MPa, which is greater than the strength shown in a previous work (82 MPa), even though the polysiloxane content and pyrolysis temperature of both samples were the same [21]. The average particle size of SiC powders of the previous work was 0.7 μm, whereas that of the present work was ~0.45 μm. The improved strength of the SC sample in the present work was caused by the finer particle size of the starting SiC powder, as was observed previously [21].

There are a few reports showing the strength of PDC-bonded SiC ceramics. The double ring strength of porous SiOC-bonded SiC ceramics pyrolyzed at 1000 °C was 2–15 MPa depending on the porosity and silicone resin type [6]. The flexural strength of polycarbosilane-derived Si(O)C bonded SiC ceramics pyrolyzed at 1100 °C was 3–16 MPa depending on the polycarbosilane content [19]. The flexural strength of the polysiloxane resin-derived ceramic-bonded SiC pyrolyzed at 1200 °C was 3–22 MPa depending on the SiC particle size and resin content [20]. In contrast, typical flexural strengths of the present SiOC-bonded SiC ceramics pyrolyzed at 800 °C ranged from 105 MPa to 153 MPa depending on the AE composition. The superior strength of the AE-modified, SiOC-bonded SiC ceramics fabricated in this study was attributed to the higher relative density (83–85%), relatively high carbon content (11.5%) [31] in the polysiloxane-derived SiOC, and beneficial effect of AE element incorporation in the SiOC bonding phase. According to Soraru et al. [11], the flexural strength of SiOC glasses increased with increasing carbon in the SiOC phase.

The present results demonstrate that (1) stronger bonding between SiC and polysiloxane-derived SiOC can be obtained by incorporating AE elements into SiOC, and (2) SiOC-bonded SiC ceramics with a flexural strength

of >150 MPa and a 16% porosity can be processed at a temperature as low as 800 °C without an applied pressure by incorporating 1% Ba-alkoxide into SiOC.

3.1.1. Effect of barium content

Because the SC–1Ba sample showed the highest strength among the samples investigated, Ba-modified SiOC-bonded SiC samples were fabricated with variations in Ba content from 0.5 to 20 mol% in polysiloxane-derived SiOC.

Fig. 4 shows the XRD patterns of selected samples pyrolyzed at 800 °C. The SC and SC–1Ba samples consisted of α-SiC (6H polytype), indicating that the polysiloxane-derived SiOC and Ba-modified polysiloxane-derived SiOC are amorphous. However, the SC–20Ba sample consisted of α-SiC and traces of BaO and $BaSiO_3$ phases. The results suggest that the Ba ion is incorporated into the SiOC structure to some extent, and Ba ions in excess of the solubility limit in polysiloxane-derived SiOC glass are precipitated as crystalline BaO and $BaSiO_3$ phases, as evidenced by XRD.

Fig. 5 shows the variation of the density and flexural strength as a function of the Ba/(Ba+Si) mole ratio in the bonding phase. The samples have the same total amount of bonding phase (20 wt%), with the Ba/(Ba+Si) ratio ranging from 0 to 0.2. The highest density and strength were obtained for a Ba/(Ba+Si) ratio of 0.01. The increase in Ba content in the polysiloxane-derived SiOC increased both properties and showed a maximum at a ratio of 0.01, beyond which the properties decrease. The incorporation of Ba ions in the polysiloxane-derived SiOC glass was beneficial for improving the density and flexural strength up to 1 mol%, indicating the 0.5 mol% or 1 mol% Ba-modified SiOC glass produces stronger bonding than SiOC glass without Ba ion between the SiC particles. However, beyond the 1 mol% Ba content, the SiOC glass becomes a more open structure, and secondary phases, such as BaO and $BaSiO_3$, are precipitated out of the glass, resulting in

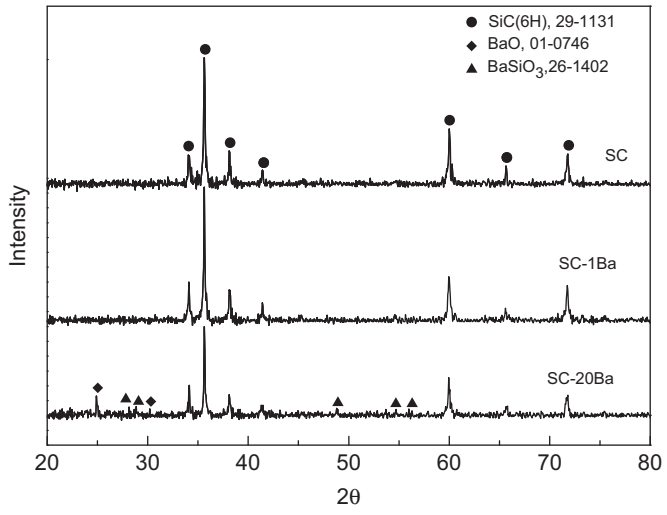

Fig. 4. XRD patterns of selected polysiloxane-derived SiOC-bonded SiC ceramics pyrolyzed at 800 °C for 2 h in nitrogen.

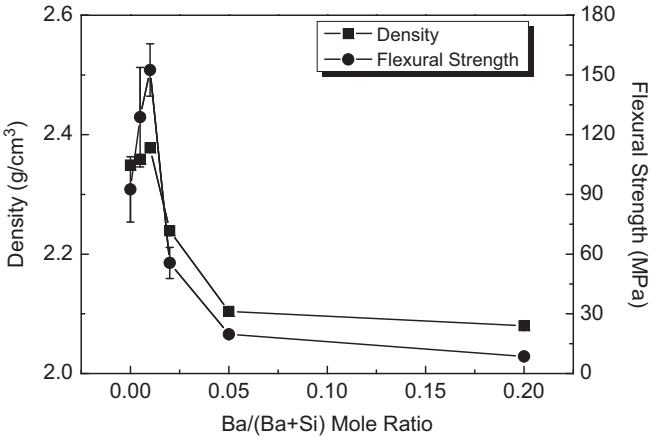

Fig. 5. Density and flexural strength of the polysiloxane-derived SiOC-bonded SiC ceramics as a function of Ba/(Ba+Si) mole ratio at constant 20 wt% bonding phase content.

weakening of the bonding between SiC particles. As a result, there is a decrease in the flexural strength, as shown in Fig. 5.

Fracture surfaces of selected samples at a lower magnification than Fig. 2 are shown in Fig. 6. The addition of 1 mol% Ba (Fig. 6(b)) produced denser material than SC material without Ba (Fig. 6(a)). However, the SC–20Ba sample contained some large pores (5–20 μm diameter), which were not observed in the other samples. The large pores may originate from the agglomerates of the added Ba-alkoxide. The significant addition of Ba-alkoxide into the polysiloxane resulted in difficulties with homogeneous mixing of the raw materials in our processing conditions. However, with the exception of the large pores, there was a more porous structure, which is consistent with the density measurement shown in Fig. 5.

The flexural strengths of the samples with or without Ba as a function of porosity are shown in Fig. 7. The SC–0.5Ba and SC–1Ba samples showed greater strength and slightly lower porosity than the SC sample without Ba. Additional Ba decreased the flexural strength and increased the porosity of Ba-modified, SiOC-bonded SiC ceramics. These results suggest that there is an optimum Ba content in the modification of SiOC glass as a bonding phase for SiC. In this case, 1 mol% Ba in the polysiloxane-derived SiOC is optimal for densification and strengthening of SiOC-bonded SiC ceramics when processed at a temperature as low as 800 °C.

3.1.2. Role of barium in silicon oxycarbide bonding phase

As shown in Fig. 8(a), we investigated the FT-IR spectra of SiOC-bonded SiC ceramics with and without Ba-alkoxide in order to characterize the bond formation. Unfortunately, it is difficult to observe a specific peak corresponding to the Si–O–Ba bond for the sample with Ba-alkoxide, which may be due to the high content of SiC in the ceramics. Fig. 8(b) presents the FT-IR spectra of only SiOC with 1% Ba-alkoxide (SiOC-1Ba) pyrolyzed at different temperatures.

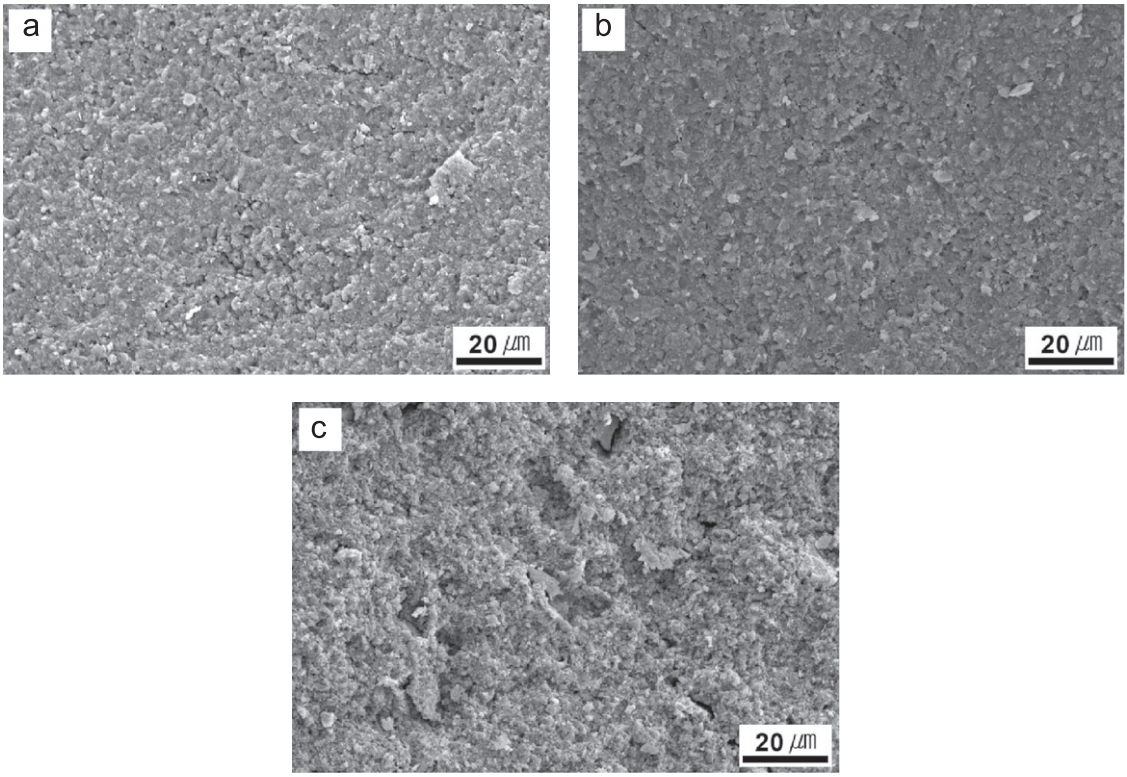

Fig. 6. Effect of Ba content on the fracture surfaces of the polysiloxane-derived SiOC-bonded SiC ceramics: (a) SC, (b) SC–1Ba, and (c) SC–20Ba (refer to Table 1).

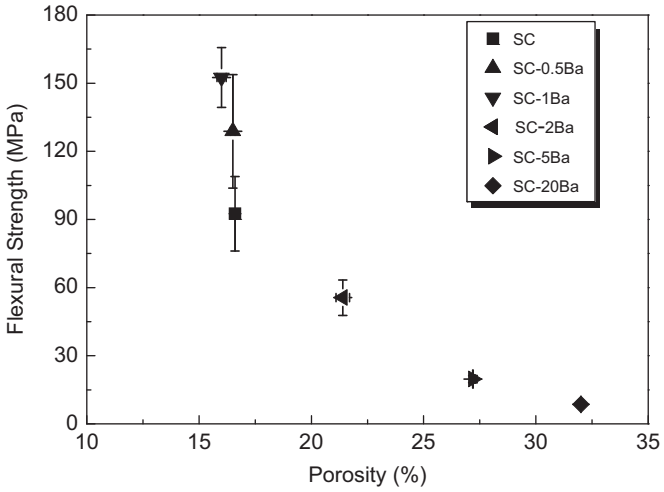

Fig. 7. Flexural strength as a function of the porosity of the Ba-modified SiOC-bonded SiC ceramics.

The 700 °C-pyrolyzed SiOC sample shows peaks at 2976 and 1275 cm^{-1}, which are assigned to C–H_3 and SiC–H_3, respectively [24,39,40]. These peaks are reduced in the 800 °C sample as a result of ceramization [24,41,42]. The peak of C–H_2 at 2922 cm^{-1} occurs in the 800 °C sample and in the 900 °C sample, indicating the formation of Si–CH_2–Si [40,43]. The broad and intense peak from 1250 to 900 cm^{-1} is related to the three kinds of Si–O–Si bonds [40]. The tiny peak at 880 cm^{-1} for the 700 and 800 °C samples is assigned to Si–O–Ba bonding [44]. The other peak near 800 cm^{-1} corresponds to Si–C bonds [40,45]. The FT-IR spectra of SiOC ceramics with different Ba-alkoxide contents were confirmed to determine the effect of Ba-alkoxide in the SiOC as the bonding phase (Fig. 8(c) and (d)). The SiOC–20Ba and SiOC–80Ba samples (Table 2) show clearer peaks at 880 cm^{-1} for the Si–O–Ba bond than SiOC–1Ba sample. Interestingly, the SiOC–1Ba sample shows Si–O–Si peaks with different shapes, ranging from 1250 to 900 cm^{-1}, compared to the SiOC sample without Ba-alkoxide (SiOC in Table 2), which has a broad peak for Si–O–Si bonds. SiOC–1Ba has a peak at 1040 cm^{-1}, as shown Fig. 8(d). It is possible for three kinds of Si–O–Si bonds to exist in SiOC ceramics as a result of different process conditions. The Si–O–Si (angle 150°) bond in the cage structure is active at 1140 cm^{-1}, the Si–O–Si (angle 144°) bond in the network structure is active at 1065 cm^{-1}, and the Si–O–Si (angle $< 144°$) bond in silicon suboxide is active at 1035 cm^{-1} [40]. Thus, SiOC–1Ba may enhance the formation of a compact silicon suboxide structure mimicking the ceramic material rather than the cage structure similar to organic–inorganic hybrid material, potentially improving the strength of the SC–1Ba sample (see Fig. 5).

4. Conclusions

By modifying commercially-available polysiloxane-derived SiOC with alkaline earth (AE) elements (Mg, Ca, Sr, Ba), SiOC-bonded SiC ceramics with improved strength were

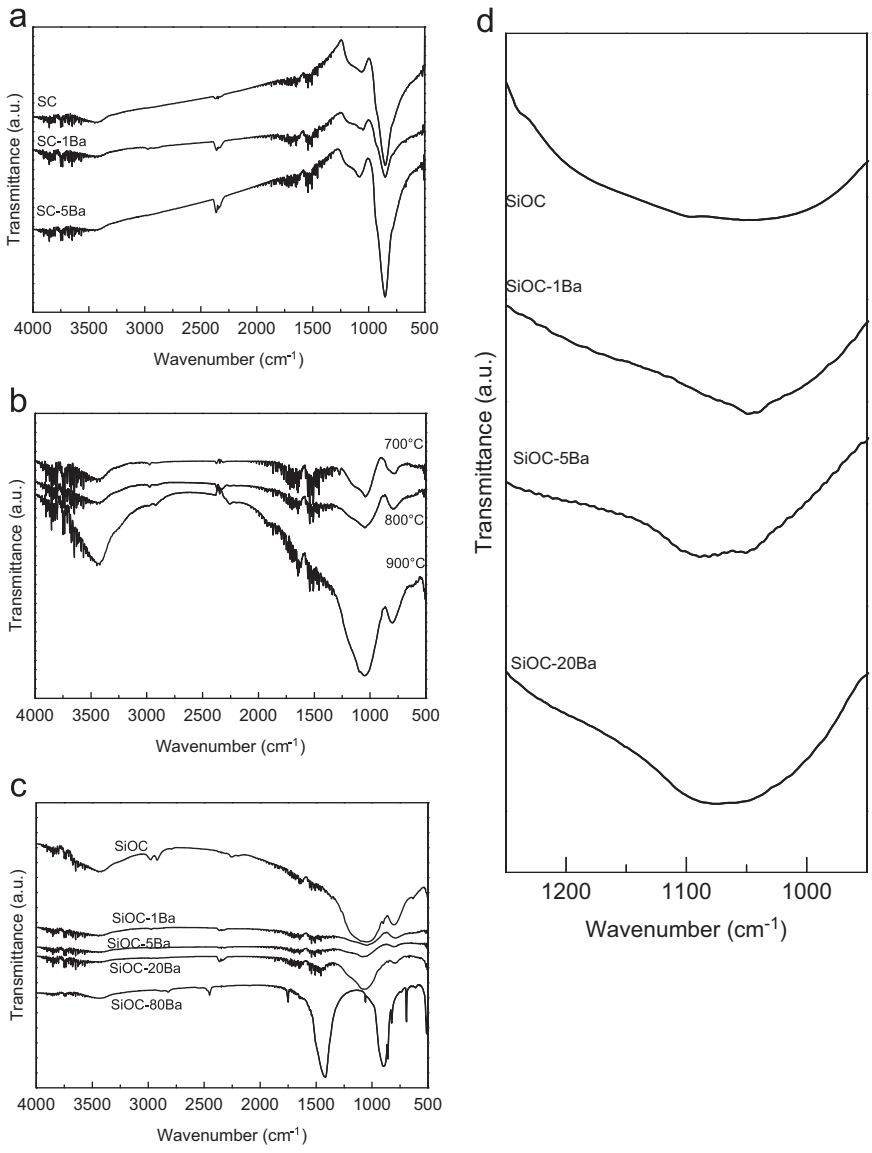

Fig. 8. FT-IR spectra of (a) SiOC-bonded SiC ceramics with and without Ba-alkoxide pyrolyzed at 800 °C, (b) SiOC ceramics containing 1% Ba-alkoxide (SiOC–1Ba) pyrolyzed at 700–900 °C, (c) and (d) SiOC ceramics containing different Ba contents pyrolyzed at 800 °C.

successfully fabricated from SiC–polysiloxane–AE alkoxide mixtures by a simple pressing and heat-treatment process at a temperature as low as 800 °C.

In Ba-modified SiOC-bonded SiC ceramics, the density and flexural strength are maximized when the Ba/(Ba + Si) mole ratio is adjusted to 0.01, which was due to the formation of both Si–O–Ba bonds and a compact silicon suboxide structure in the bonding phase. The porosity and flexural strength of the material at room temperature were 16% and 153 MPa, respectively.

The present results demonstrate that (1) stronger bonding between SiC and polysiloxane-derived SiOC can be obtained by incorporating AE elements into SiOC, (2) there is an optimum AE elements content at which optimum mechanical properties were realized, and (3) excess Ba beyond the solubility limit in SiOC glass forms crystalline BaO and $BaSiO_3$ phases, which deteriorate the mechanical properties of SiOC-bonded SiC ceramics.

Acknowledgment

This work was supported by the 2011 Research Fund of the University of Seoul.

References

[1] G.D. Soraru, S. Modena, E. Guadagnino, P. Colombo, J. Egan, C. Pantano, Chemical durability of silicon oxycarbide glasses, Journal of the American Ceramic Society 85 (2002) 1529–1536.

[2] J. Latournerie, P. Dempsey, D. Hourlier-Bahloul, J.P. Bonnet, Silicon oxycarbide glasses: Part 1—thermochemical stability, Journal of the American Ceramic Society 89 (2006) 1485–1491.

[3] T. Xu, Q. Ma, Z. Chen, High-temperature behavior of silicon oxycarbide glasses in air environment, Ceramics International 37 (2011) 2555–2559.
[4] G.D. Soraru, L. Pederiva, J. Latournerie, R. Raj, Pyrolysis kinetics for the conversion of a polymer into an amorphous silicon oxycarbide ceramic, Journal of the American Ceramic Society 89 (2002) 2181–2187.
[5] A. Klonczynski, G. Schneider, R. Riedel, R. Theissmann, Influence of boron on the microstructure of polymer derived SiCO ceramics, Advanced Engineering Materials 6 (2004) 64–68.
[6] M. Thunemann, A. Herzog, U. Vogt, O. Beffort, Porous SiC-preforms by integranular binding with preceramic polymers, Advanced Engineering Materials 6 (2004) 167–172.
[7] T. Varga, A. Navrotsky, J.L. Moats, R.M. Morcos, F. Poli, K. Muller, A. Saha, R. Raj, Thermodynamically stable $Si_xO_yC_z$ polymer-like amorphous ceramics, Journal of the American Ceramic Society 90 (2007) 3213–3219.
[8] X. Yuan, S. Chen, X. Zhang, T. Jin, Joining SiC ceramics with silicon resin YR3184, Ceramics International 35 (2009) 3241–3245.
[9] P. Colombo, G. Mera, R. Riedel, G.D. Soraru, Polymer-derived ceramics: 40 years of research and innovation in advanced ceramics, Journal of the American Ceramic Society 93 (2010) 1805–1837.
[10] B.V.M. Kumar, Y.W. Kim, Processing of polysiloxane-derived porous ceramics: a review, Science and Technology of Advanced Materials 11 (2010) 044303.
[11] G.D. Soraru, E. Dallapiccola, G. D'Andrea, Mechanical characterization of sol–gel-derived silicon oxycarbide glasses, Journal of the American Ceramic Society 79 (1996) 2074–2080.
[12] S.P. Shah, R. Raj, Mechanical properties of a fully dense polymer derived ceramic made by a novel pressure casting process, Acta Materialia 50 (2002) 4093–4103.
[13] M. Esfehanian, R. Oberacker, T. Fett, M.J. Hoffmann, Development of dense filler-free polymer-derived SiOC ceramics by field-assisted sintering, Journal of the American Ceramic Society 91 (2008) 3803–3805.
[14] S. Martinez-Crespiera, E. Ionescu, H.J. Kleebe, R. Riedel, Pressureless synthesis of fully dense and crack-free SiOC bulk ceramics via photo-crosslinking and pyrolysis of a polysiloxane, Journal of the European Ceramic Society 31 (2011) 913–919.
[15] P. Colombo, J.R. Hellmann, D.L. Shelleman, Thermal shock behavior of silicon oxycarbide foams, Journal of the American Ceramic Society 85 (2002) 2306–2312.
[16] T. Rouxel, G.D. Soraru, J. Vicens, Creep viscosity and stress relaxation of gel-derived silicon oxycarbide glasses, Journal of the American Ceramic Society 84 (2001) 1052–1058.
[17] A. Scarmi, G.D. Soraru, R. Raj, The role of carbon in unexpected visco(an)elastic behavior of amorphous silicon oxycarbide above 1273 K, Journal of Non-Crystalline Solids 351 (2005) 2238–2243.
[18] G.D. Soraru, R. Campostrini, S. Maurina, F. Babonneau, Gel precursor to oxycarbide glasses with ultrahigh ceramic yield, Journal of the American Ceramic Society 80 (1997) 999–1004.
[19] S. Zhu, S. Ding, H. Xi, R. Wang, Low-temperature fabrication of porous SiC ceramics by preceramic polymer reaction bonding, Materials Letters 59 (2005) 595–597.
[20] Y. Ma, Q.S. Ma, J. Suo, Z.H. Chen, Low-temperature fabrication and characterizaton of porous SiC ceramics using silicone resin as binder, Ceramics International 34 (2008) 253–255.
[21] J.H. Eom, Y.W. Kim, Low-temperature processing of silicon oxycarbide-bonded silicon carbide, Journal of the American Ceramic Society 93 (2010) 2463–2466.
[22] T. Erny, M. Seibold, O. Jarchow, P. Greil, Microstructure development of oxycarbide composites during active-filler-controlled polymer pyrolysis, Journal of the American Ceramic Society 76 (1993) 207–213.
[23] G.D. Soraru, G. D'Andrea, R. Campostrini, F. Babonneau, G. Mariotto, Structural characterization and high-temperature behavior of silicon oxycarbide glasses prepared from sol–gel precursors containing Si–H bonds, Journal of the American Ceramic Society 78 (1995) 379–387.
[24] R. Harshe, C. Balan, R. Riedel, Amorphous Si(Al)OC ceramic from polysiloxanes: bulk ceramic processing, crystallization behavior and applications, Journal of the European Ceramic Society 24 (2004) 3471–3482.
[25] L. Toma, C. Fasel, S. Lauterbach, H.J. Kleebe, R. Riedel, Influence of nano-aluminum filler on the microstructure of SiOC ceramics, Journal of the European Ceramic Society 31 (2011) 1779–1789.
[26] M. Fukushima, E. Yasuda, Y. Nakamura, M. Shimizu, Y. Teranishi, L.M. Manocha, Y.J. Tanabe, Oxidation behavior of Si–Nb–C–O ceramics prepared by the pyrolysis of methyltriethoxysilane based organic-inorganic hybrid gel, Journal of Sol–Gel Science and Technology 34 (2005) 15–21.
[27] E. Ionescu, B. Papendorf, H.J. Kleebe, F. Poli, K. Muller, R. Riedel, Polymer-derived silicon oxycarbide/hafnia ceramic nanocomposites. Part I: phase and microstructure evolution during the ceramization process, Journal of the American Ceramic Society 93 (2010) 1774–1782.
[28] E. Ionescu, B. Papendorf, H.J. Kleebe, R. Riedel, Polymer-derived silicon oxycarbide/hafnia ceramic nanocomposites. Part II: stability toward decomposition and microstructure evolution at $T \gg 1000\ ^\circ C$, Journal of the American Ceramic Society 93 (2010) 1783–1789.
[29] L. Bergero, V.M. Sglavo, G.D. Soraru, Processing and thermal shock resistance of a polymer-derived $MoSi_2$/SiCO ceramic composites, Journal of the American Ceramic Society 88 (2005) 3222–3225.
[30] J. Liu, L. Zhang, Q. Liu, L. Cheng, Y. Wang, Polymer-derived SiOC–barium–strontium aluminosilicate coatings as an environmental barrier for C/SiC composites, Journal of the American Ceramic Society 93 (2010) 4148–4152.
[31] Y.W. Kim, S.H. Kim, I.H. Song, H.D. Kim, C.B. Park, Fabrication of open-cell, microcellular silicon carbide ceramics by carbothermal reduction, Journal of the American Ceramic Society 88 (2005) 2949–2951.
[32] M. Narisawa, H. Yasuda, R. Mori, H. Mabuchi, K. Oka, Y.W. Kim, Silicon carbide particle formation from carbon black-polymethylsilsesquioxane mixtures with melt pressing, Journal of the Ceramic Society of Japan 116 (2008) 121–125.
[33] T. Rouxel, J.C. Sangleboeuf, J.P. Guin, V. Keryvin, G.D. Soraru, Surface damage resistance of gel-derived oxycarbide glasses: hardness, toughness, and scratchability, Journal of the American Ceramic Society 84 (2001) 2220–2224.
[34] P. Colombo, V. Sglavo, E. Pippel, J. Woltersdorf, Joining of reaction-bonded silicon carbide using a preceramic polymer, Journal of Materials Science 33 (1998) 2405–2412.
[35] L.J. Gibson, M.F. Ashby, in: Cellular Solids, Cambridge University Press, Cambridge, 1999, pp. 210–214.
[36] R.W. Rice, Comparison of stress concentration versus minimum solid area based mechanical property–porosity relations, Journal of Materials Science 28 (1993) 2187–2190.
[37] J.H. Eom, Y.W. Kim, I.H. Song, Effects of the initial α-SiC content on the microstructure, mechanical properties, and permeability of macroporous silicon carbide ceramics, Journal of the European Ceramic Society 32 (2012) 1283–1290.
[38] J.Y. Kim, Y.W. Kim, M. Mitomo, G.D. Zhan, J.G. Lee, Microstructure and mechanical properties of α-silicon carbide sintered with yttrium–aluminum garnet and silica, Journal of the American Ceramic Society 82 (1999) 441–444.
[39] N. Takamura, K. Taguchi, T. Gunji, Y. Abe, Preparation of silicon oxycarbide ceramic films by pyrolysis of polymethyl- and polyvinylsilsesquioxanes, Journal of Sol–Gel Science and Technology 16 (1999) 227–234.
[40] A. Grill, D.A. Neumayer, Structure of low dielectric constant to extreme low dielectric constant SiCOH films: Fourier transform infrared spectroscopy characterization, Journal of Applied Physics 94 (2003) 6697–6707.
[41] P.H. Mutin, Control of the composition and structure of silicon oxycarbide and oxynitride glasses derived from polysiloxane precursors, Journal of Sol–Gel Science and Technology 14 (1999) 27–38.

[42] R. Pena-Alonso, L. Tellez, A. Tamayo, F. Rubio, J. Rubio, J.L. Oteo, Silicon–titanium oxycarbide glasses as bimodal porous inorganic membranes, Journal of the European Ceramic Society 27 (2007) 969–973.
[43] A. Castex, L. Favennec, V. Jousseaume, J. Bruat, J. Deval, B. Remiat, G. Passemard, M. Pons, Study of plasma mechanisms of hybrid α-SiOC:H low-*k* film deposition from decamethylcyclopentasiloxane and cyclohexene oxide, Microelectronic Engineering 82 (2005) 416–421.
[44] M. Handke, M. Urban, IR and Raman spectra of alkaline earth metals orthosilicates, Journal of Molecular Structure 79 (1982) 353–356.
[45] G.M. Renlund, S. Prochazka, R.H. Doremus, Silicon oxycarbide glasses: Part II—structure and properties, Journal of Materials Research 6 (1991) 2723–2734.